Summary of Natural Convection and the Rayleigh Problem

Bruce A. Finlayson
Rehnberg Professor Emeritus of Chemical Engineering
University of Washington, Seattle,WA
June, 2013

This write-up describes natural convection and the transition from no flow, to laminar flow, to transient laminar flow, to soft turbulence and then hard turbulence as the temperature difference increases when a fluid layer is contained between two flat plates, heated from below. Both experimental and theoretical information is summarized.

The material is from the final report of a research grant (Feb., 2000)

Bruce A. Finlayson
ChemEComp@gmail.com

Author of *Introduction to Chemical Engineering Computing*,
Wiley (2006; 2nd ed., 2012)
www.ChemEComp.com

Finally, some simulations done with various turbulence models for natural convection are summarized.

Rayleigh Problem

The Rayleigh problem is a classic problem: find the heat transfer across a horizontal layer of fluid when the bottom plate is heated and the top plate is cooled. Basically, what has been found is that the heat transfer takes place by conduction until a critical Rayleigh number is reached. The Rayleigh number is

$$Ra = \frac{\rho^2 \beta g C_p L^3 \Delta T}{\mu k}, \quad Pr = \frac{C_p \mu}{k}, \quad Ra = Gr\ Pr$$

where ΔT is the temperature difference across the layer of thickness L, and the critical value is 1708. Note that the Rayleigh number can be increased for the same fluid by increasing the temperature difference across the layer. When that is done, it is found that at higher Rayleigh number the flow pattern changes at discrete values of Rayleigh number. The laminar transitions were first found by Malkus and Veronis (1958). Here we concentrate on higher Rayleigh numbers leading to transient flows. (Incidently, the Rayleigh problem is often called the Rayleigh-Bénard problem. This is inappropriate since Bénard's experiments are clearly surface tension driven rather than buoyancy driven.)

Consider the experiment done by Heslot, *et al.* (1987). This is not a classic Rayleigh problem, but it shows all the same features very clearly and the experiment can be done at higher values of Rayleigh number. Helium is placed in the cylindrical vessel, which is insulated on the sides. By changing the pressure and the temperature difference , it is possible to cover a range in Rayleigh number from 2000 to 10^{11}. For this geometry, the onset of convection is at Ra = 5,800. Thus, for Ra lower than this, no motion occurs and the Nusselt number is 1.0 (representing conduction only). For Ra between 5,800 and 90,000 laminar, steady convection takes place, and the Nusselt number increases with Ra, as shown in the Figure 6.5.

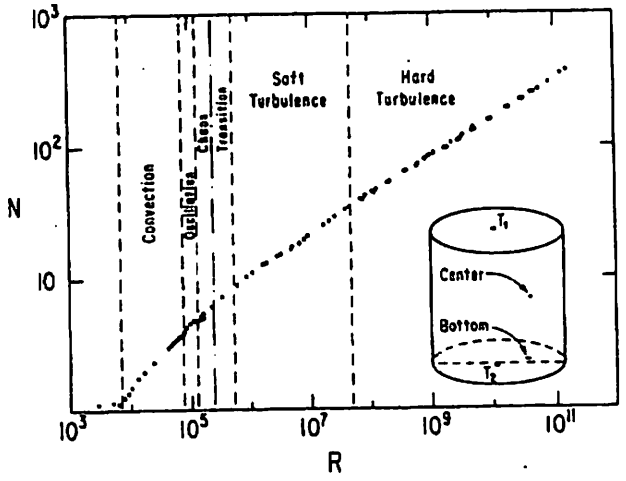

Figure 6.5. Nusselt Number versus Rayleigh Number, Heslot, *et al.* (1987). The experimental cell has a height and diameter of 8.7 cm.

For Ra between 90,000 and 150,000 a laminar convection takes place, but it is oscillatory with regular periods. For Ra between 150,000 and 2.5 x 10^5 the flow is chaotic. For Ra between 2.5 x 10^5 and 4 x 10^7 'soft' turbulence occurs. This regime is when a boundary layer forms on the sides and the vertical length scale no longer matters. In this region, the Nusselt number is given by

$$Nu = 1 + 0.096\ Ra^{0.333}, \quad 2.5 \times 10^5 < Ra < 4 \times 10^7$$

For Ra between 4 x 10^7 and 10^{11} 'hard' turbulence occurs. This regime is when the turbulent boundary layer is interrupted with abrupt detachment of plumes which push into the central core. In this region, the Nusselt number is given by

$$Nu = 1 + 0.2\ Ra^{0.282}, \quad 4 \times 10^7 < Ra < 10^{11}$$

While not stated in this article, a later article by the same authors (Castaing, *et al.* 1989) gives the Prandtl number as varying between 0.65 and 1.5 in these experiments. It isn't constant because the temperature and pressure are both changing, but it is relatively constant. These experiments are also done for a small aspect ratio, since the height equals the diameter of the cylinder.

In a later paper, the same authors increased the range of Rayleigh number to 6 x 10^{12}. They find that the Nusselt number obeys the formula

$$Nu = (0.23 \pm 0.03)\ Ra^{0.282 \pm 0.006}$$

Simulations of the regime of 'hard' turbulence have been done by Kerr (1996) using direct numerical simulation. They did calculations for air (Pr = 0.7) with Ra between 5 x 10^4 and 2 x 10^7. His simulations were for a geometry with the ratios 6:6:1, where the height is the 1. The important point about these simulations is that he had to use 96 Chebyshev orthogonal polynomials

in the vertical direction and a Fourier method in the horizontal directions, using 128 x128 Fourier modes. The calculation for Ra = 2 x 10^7 took 400 hours on a CRAY Y-MP. Basically, the mesh size needed to be smaller than the Kolmogorov scale of turbulence (about 30 μm for pipe flow) for the direct simulations to be successful.

Kadanoff (1991) provide a summary of results. His picture of the structure in the 'hard' turbulence region is shown in the Figure 6.6.

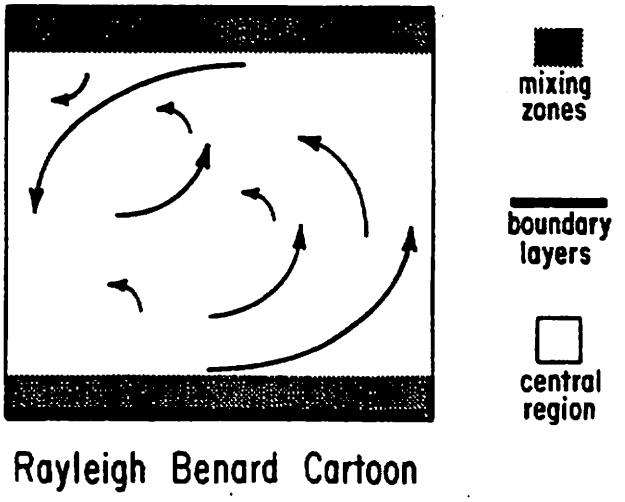

Figure 6.6. Sketch of Rayleigh Convection, Kadanoff (1991)

The thickness of the boundary layer scales with Rayleigh number as

$$\frac{\lambda}{L} = Ra^{-2/7}$$

and the mixing zone scale as scales with Rayleigh number as

$$\frac{d_m}{L} = Ra^{-1/7}$$

For Ra = 10^7 we have

$$\frac{\lambda}{L} = 0.01, \frac{d_m}{L} = 0.1$$

Thus, the boundary layer covers 1% of the distances of the top and bottom, the mixing zone covers 10% of the distance of the top and bottom, and the central core (relatively uniform temperature) covers 78% of the region.

An earlier computational effort (McLaughlin and Orszag, 1982) gave results which disagree with the experiments given above. They predicted that the transition to chaotic convection occurs

for Rayleigh numbers larger than about 9000. The experiments of Heslot, et al. (1987) give that value as 150,000. While the geometries are not quite comparable, this comparison shows the importance of using the latest computational techniques. McLaughlin and Orszag do, however, give a good qualitative description of the flow, which is repeated here.

> "One must be cautious about using the word 'turbulent' to describe these freely convecting flows since this word is usually associated with high-Reynolds-number flows, such as fully developed turbulent pipe flow, in which the energy is distributed over a large range of spatial and temporal scales. The kind of convective flows which we shall discuss in this paper typically have Reynolds numbers (based on the maximum velocity and the thickness of the convection layer) of order 10-100, and have over 99% of their kinetic energy contained in a single octave of wavenumbers. Thus one should not confuse the kind of weak turbulence which we shall discuss with, for example, the kind of strong turbulence encountered in pipe flow and analyzed in the classic experiments of Laufer (1954). Nevertheless, the convective processes studied here are of interest since they give an example of one way fluid flow can become chaotic."

Prasad (1999) used direct numerical simulation to study a fluid layer heated from below. Turbulence was present at $Ra = 2 \times 10^7$, which was analyzed using a 96 x 96 x 128 grid. The calculations took 3.3 hours of CRAY J90 time to simulate 0.16 hours of physical time.

Thermally-driven Cavity Problem

The thermally-driven cavity problem is one for which there is an enhancement of the rate of heat transfer for any Rayleigh number, defined now in terms of the distance between the two vertical surfaces and the temperature difference between them. This result follows from the fact that natural convection will occur anytime the temperature gradient has a component not aligned with gravity.

Ivey (1984) did experiments in which he measured the temperature fluctuations. He found that the motion oscillated in time but gradually approached steady state for $Pr = 7.1$ and $Ra = 9.2 \times 10^8$, and for $Pr = 6.6$ and $Ra = 1.2 \times 10^9$, all with an aspect ratio of 1. The case with $Pr = 7.1$ and $Ra = 9.2 \times 10^8$, though, approached the steady state in a monotone fashion, as shown in Figure 6.7.

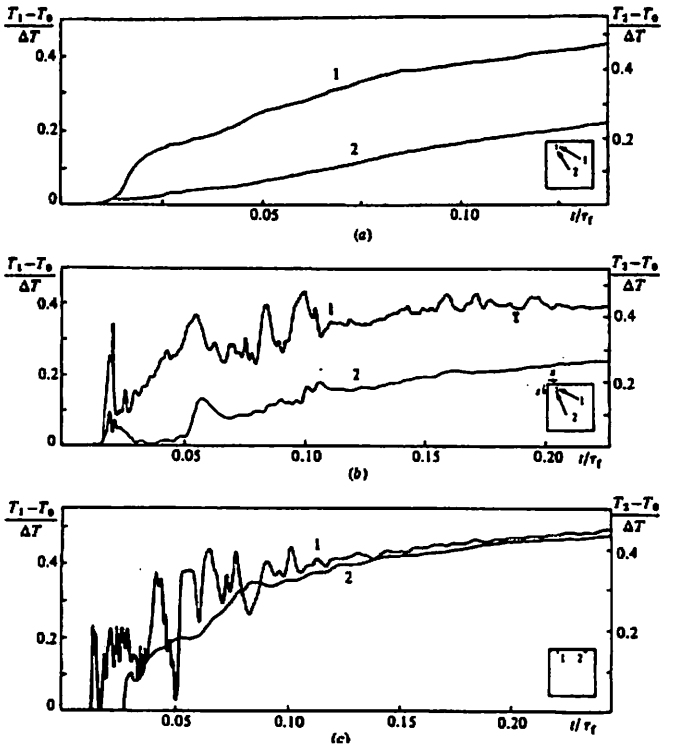

Figure 6.7. Temperature traces, A = 1. (a) Ra = 3.9 x 10^8, Pr = 82; (b) Ra = 9.2 x 10^8, Pr = 7.1; (c) Ra = 1.2 x 10^9, Pr = 6.6; Ivey (1984)

Gebhart, et al. (1988) report that Elder (1965) did experiments with silicone oil (Pr = 1000) and found secondary flows began at Re = 3 x 10^5, tertiary flows arose for Re greater than 10^6, and turbulence began at Ra = 2 x 10^9.

Paolucci and Chenoweth (1989) did direct numerical simulation using a 121 x 121 non-uniform mesh. For air (Pr = 0.71), and an aspect ratio, A, of 1.0, they found the following transient phenomena. For Rayleigh numbers up to 2 x 10^8 the flow was strictly periodic; then up to 3 x 10^8 it was quasi-periodic; then up to 4 x 10^8 it was non-periodic; finally up to 10^{10} it was fully turbulent. The time histories of the temperatures in these various cases are shown in the Figure 6.8. The phase space trajectory of temperature versus one velocity component are shown in the next Figure 6.9.

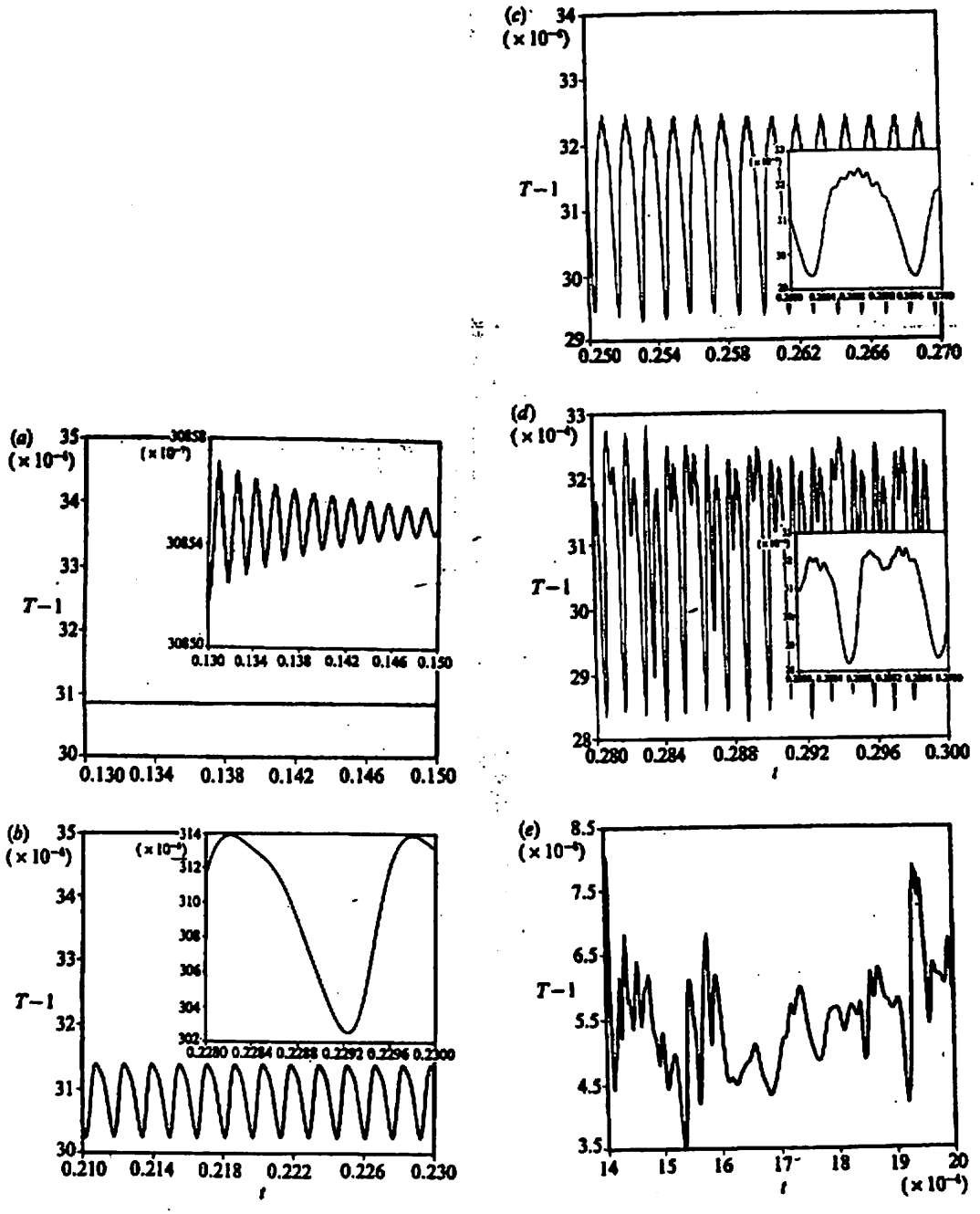

Figure 6.8. Temperature time histories, A = 1; (a) Ra = 1.9 x 10^8; (b) Ra = 2.0 x 10^8; (c) Ra = 3.0 x 10^8; (d) Ra = 4.0 x 10^8; (e) Ra = 10^{10}; Paolucci and Chenoweth (1989)

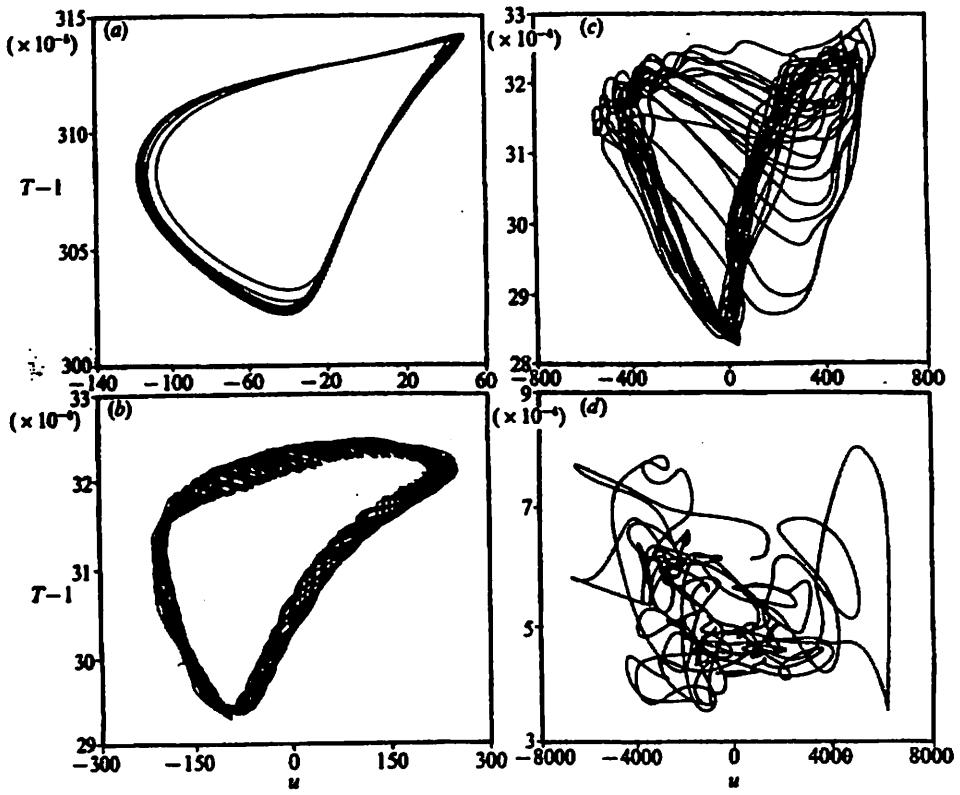

Figure 6.9. Phase space trajectory of temperature versus velocity component u for A = 1; Paolucci and Chenoweth (1989). (a) Ra = 2 x 10^8; (b) Ra = 3 x 10^8; (c) Ra = 4 x 10^8; (d) Ra = 10^{10};

This figure clearly shows the periodic behavior at the lowest Ra, then as the Ra is increased it shows the quasi-periodic behavior, then the chaotic behavior. These authors argue that there are two modes to the instability. One of them arises at the corners and results in internal waves; this is called Ra_{ci}. The other arises in the thermal boundary layers along the heated wall; this is called Ra_{cw}. The corner instability generally occurs first when the aspect ratio is small, and the boundary layer instability occurs first when the aspect ratio is large. The formulas for these critical values are

$$Ra_i = 1.93 \times 10^8 \, A^{-3.15}$$

$$Ra_w = 2.70 \times 10^8 \, A^{-2.75}$$

Figure 6.10 shows the dependence of the two critical Rayleigh numbers on the aspect ratio. To the right of the curves the perturbations to the motion are amplified and they are oscillatory, and to the left of the curves perturbations to the motion are damped.

For an aspect ratio of A = 1 the critical Ra is 1.93 x 10^8. For aspect ratios above 3, the first instability from steady flow is due to the sidewall boundary layer. For aspect ratios smaller than that but greater than 0.5, the first instability from steady flow is due to internal waves at the

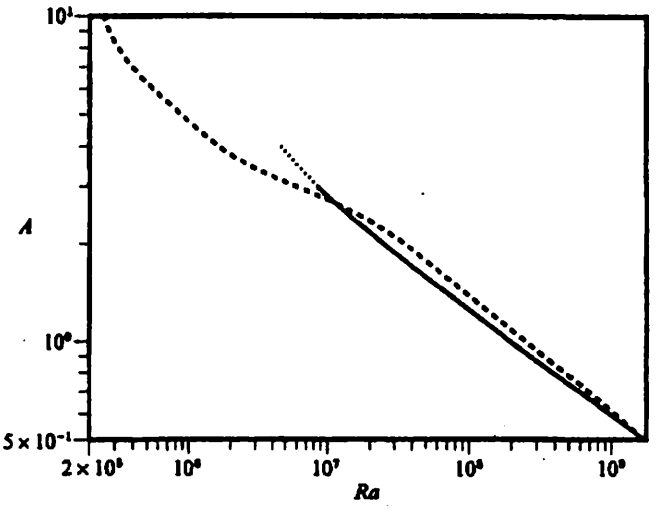

Figure 6.10. Critical Rayleigh number as a function of aspect ratio, ____ Ra_i; - - - -Ra_w; Paolucci and Chenoweth (1989)

corners. Above the first critical Ra both phenomena can occur. The authors report that their calculations did not die away in the same circumstance in which Ivey (1984) measured them dying away. They indicate that this is due to the Prandtl number. Paolucci and Chenoweth (1989) do calculations for air, Pr = 0.71, whereas Ivey (1984) did experiments for water, Pr = 7.1. Thus Paolucci and Chenoweth (1989) did one calculation for Pr = 7.1. They found that the internal wave instability behaved as Ivey measured it (it approached a steady state), and indeed so did the boundary layer instability. The flow seemed to approach a steady state in the same time period used by Ivey (1984) in the experiment. When they continued the calculation for a longer time, however, they found that the boundary layer instability started. This point illustrates another difficulty of these calculations: when the solution is slowly changing, is it slowing converging to a steady state situation, or will it become transient if the calculation is continued further.

Henkes and Hoogendoor (1990) did calculations for Pr = 0.71, resulting in a critical value of Ra = 2 x 10^8 separating steady from transient flows , and for Pr = 7.0, resulting in a critical value of Ra = 4 x 10^9 separating steady from transient flows. That is, for Ra below 4 x 10^9 the flow converges to a steady flow in an oscillating way. They point out that Ivey (1984) obtained the same behavior for Ra up to 1.2 x 10^9, but didn't do experiments at higher Ra. Thus, theory and experiment can be compared for Ra $\leq$ 1.2 x 10^9, and they agree. They also say that water does not show the same instability in the corner that air does. For water, the instability occurs in the boundary layer. Thus, which type of instability occurs first also depends on Prandtl number.

A number of other articles have presented calculations which help to identify the mesh sizes needed to solve these problems. Le Quéré (1991) solved numerically for Ra = 10^6, 10^7, and 10^8 (all steady solutions). They obtained Nusselt numbers of 8.825, 16.523, and 30.225, respectively. His calculations used a pseudo-spectral Chebyshev method with 128 x 128 polynomial expansions.

Lage and Bejan (1991) did transient simulations using a finite volume method for Pr = 10, Ra = 10^{11}. They used a graded mesh and found that a 26 x 26 mesh was not good enough, but 52 x 52 and 104 x 104 gave similar results. To integrate to the point that the solution kept repeating itself required integrating up to $\tau = 12$, where τ is

$$\tau = t \frac{\alpha (Ra\ Pr)^{1/2}}{H^2}$$

The time step needed was $\Delta \tau = 0.016$ for the 52 x 52 mesh.

Janssen and Henkes (1993) did calculations for Pr = 0.71 using a finite volume method. They found that for Ra = 10^8 they got a transition to turbulence and full turbulence for Ra = 2 x 10^8. To do the transient calculations they used a 240 x 240 mesh or a 360 x 360 mesh, with irregular mesh spacing. These two meshes gave equivalent results.

Tagawa and Ozoe (1996) used a 55 x 55 grid for Pr = 1, Ra up to 2 x 10^7 (the flow was always steady), using a high-order finite difference method. They also did calculations for Pr = 0.025, and got oscillatory solutions for Ra = 5 x 10^5. These results again point out that the Ra for which oscillations occur changes with Prandtl number, generally increasing as the Prandtl number increases. The calculations at these Rayleigh numbers took the following times to reach steady state: $\tau = 2000$ for Pr = 1, Ra = 2 x 10^7; $\tau = 600$ for Pr = 0.025, Ra = 5 x 10^5. The definition of τ is

$$\tau = \frac{t}{t_0},\ t_0 = \frac{x_0^2}{\alpha}$$

These results give an indication of the time it takes to reach steady state.

Turbulence Models

The direct numerical simulation of turbulence in natural convection situations shows that a great many terms are needed in the time-dependent calculation. For example, even for a relatively low Ra = 5 x 10^6, it is necessary to use $(100\text{-}200)^2$ points for a 2D calculation, i.e. 10^4 to 40,000 points (Versteegh and Nieuwstadt, 1999). In 3D the computer resources are immense (for example, the one calculation taking 400 hours of a CRAY computer). These cases are for simple geometries, which is definitely not the case for the 3D transformer. Thus, other models of turbulence are considered that simply somewhat the computational task. The models discussed here are k-ε models, or variants thereof.

In a k-ε model, k represents the turbulent kinetic energy per unit mass and ε represents the rate of dissipation of turbulent kinetic energy. The turbulent viscosity and turbulent diffusivity are written in terms of these quantities. Two additional equations must be added to the Navier-Stokes equation and energy equation, and the parameters for these additional equations are chosen to make

the simulations agree with experiment. Thus, the constants themselves have to be carefully selected to model a particular situation. Here we discuss a few papers dealing with natural convection at a boundary layer next to a hot vertical plate and natural convection in a square cavity.

Henkes and Hoogendoorn (1989) compare different k-ε model for natural convection in a thermal boundary layer. They find that turbulence occurs for $Gr_x = 2 \times 10^9$ (rather than for $Re_x = 1.5 \times 10^6$ for forced convection along a vertical plate). They also give several references to articles showing that the turbulent model (with no forcing of k or ε at the walls) can give the laminar flow solution. Thus, they do not 'turn on' the turbulence in their k-ε model until $Gr_x = 2 \times 10^9$. They also find that a special, low-Reynolds number turbulence model is necessary, and find that due to Chien (1980, 1982), and Jones and Launder (1972) perform the best. The standard k-ε model can be used if it is modified using Chien's D and f_μ functions. Pironneau (1999) say that the transition to turbulence cannot be determined using a k-ε model.

Peeters and Henkes (1992) say that the k-ε model is not always good in complex geometries, and they examine a Reynolds-stress model. This model is even more complicated than the k-ε model. They also point out that different constants are needed in the k-ε model in buoyant flows than in forced flows, presumably because of the lower Reynolds number in buoyant flows. While the Reynolds-stress model does show better agreement with experimental results for the details of the turbulent flow, the k-ε model shows satisfactory agreement with the macroscopic features even though the spatial distribution of things like the turbulent kinetic energy might be incorrect.

The square cavity is different from, and more complicated than, the boundary layer flow. This is because of the interaction of the instabilities from internal waves (beginning in the corner) and the boundary layer instabilities. As shown above, which of these occurs in any situation depends on the Rayleigh number, the Prandtl number, and the aspect ratio. Henkes, *et al.* (1991) have compared low-Reynolds number k-ε models of turbulence in a square cavity. They find that the models of Chien (1980, 1982), and Jones and Launder (1972) are the best. They also clearly lay out the facts that the transition to turbulence is predicted for different Rayleigh numbers, depending on the model. Some of the models can predict laminar flow (i.e. a laminar flow is consistent with the model and especially the boundary conditions). Indeed, in these models it is sometimes necessary to 'seed' the turbulence in order for it to be the final solution. The results are as follows.

		k-ε model	Chien	Jones-Launder
Ra_{cr}, air, Pr = 0.71	10^9	10^{10}	10^{11}	
Ra_{cr}, water, Pr = 6.7	10^{11}	10^{12}	10^{13}	

This paper says that accurate experiments for the square cavity do not exist at high Rayleigh number, and that the proper wall functions are still being derived. They estimate that the number of time steps needed to approach steady state in this problem is $Ra^{1/2}$; they have a special initial

condition to reduce this to $Ra^{1/4}$. (For $Ra = 10^{14}$, these are 10^7 and 4000 steps, respectively.) Their simulations are time-dependent, but integrated on a time scale that is longer than the turbulent fluctuations. They say:

> "It seems a bit strange that, despite the time-averaging, the unsteady terms remain in the formulation. However, the time-averaging is restricted to the broad-band spectrum of turbulence, whereas the remaining unsteady terms account for all weak unsteadiness that does not belong to the turbulence. We can also define that the unsteady terms represent all unsteadiness that is not modelled by the turbulence model."

Their simulations show oscillations due to the internal gravity waves, but they die out in time.

Liu and Wen (1999) advance another model of turbulent buoyant flows. They were able to do calculations for the square cavity on a 60 x 60 graded mesh for air at a Rayleigh number of 1.58×10^9. They had to take about 2000 time steps to approach steady state.

Definition of Model Problems

The three model problems shown above will be solved using a k-ε model in FIDAP. FIDAP contains a low-Reynolds number turbulence model, called the Wilcox model. This model has not been compared with natural convection simulations, as summarized above. In fact, the reference to it is an industrial report, which may not even be available. However, it will be used with FIDAP since the standard k-ε model is not appropriate for natural convection problems. Generally, a 49 x 49 graded mesh will be used, being careful to check that there are several elements contained within any boundary layer that forms. The Rayleigh numbers to be studied are computed using the geometry of the situation, the fluid properties for a ferrofluid, and the ΔT corresponding to the maximum temperature rise that can be tolerated in a transformer minus the surrounding temperature, 125 – 25 = 100 ° C. (This is the working hypothesis, although it could be changed as calculations proceed.) The physical properties are given in Table 6.1.

Table 6.1. Preferred Physical Properties

Property	Shell Oil	Ferrofluid
density	$\rho = 849$	913 kg/m^3
viscosity	$\mu = 3.81 \times 10^{-3}$	0.00665 kg/m s
heat capacity	$Cp_f = 2038$	1922 J/kg K
thermal conductivity	$k_f = 0.122$	0.127 W/m K
thermal expansion coefficient	$\beta = 7.17 \times 10^{-4}$	$7.17 \times 10^{-4} K^{-1}$
K (A / m K)		12.

Thus, we have

$$Ra = 1.33 \times 10^{10} \Delta T L^3 \text{ for a ferrofluid, } Pr = 100.6$$

$$Ra = 2.22 \times 10^{10} \Delta T L^3 \text{ for the Shell oil, } Pr = 63.6.$$

When $\Delta T = 100$, and $L = 0.01$ m (appropriate for a duct) the Rayleigh numbers are: $Ra = 1.33 \times 10^6$ for the ferrofluid and 2.22×10^6 for the Shell oil. When $\Delta T = 100$, and $L = 0.1$ m (appropriate for the outer edge) the Rayleigh numbers are: $Ra = 1.33 \times 10^9$ for the ferrofluid and 2.22×10^9 for the Shell oil.

Summary of Known Results

There is disagreement between different authors as to the critical Rayleigh number for transition to turbulence, probably because the transition is not abrupt, but arises from instabilities that must grow before turbulence begins. For the fluid layer problem, turbulence occurs for a Rayleigh number of 2.5×10^5, but transient and chaotic flows occur for Ra between 90,000 and 2.5×10^5. A plot of the flow regimes is shown in Figure 6.11. For the heated cavity problem, several authors have calculated transition to turbulence at $Ra = 2 \times 10^8$ for fluids with $Pr = 0.71$ (air) and at $Ra = 4 \times 10^9$ for fluids with $Pr = 7$ (water). Thus, the Rayleigh number that would result in turbulenct flow in transformer elements is not known precisely, especially since the Prandtl number is much larger (between 60 and 100), which makes the present study valuable.

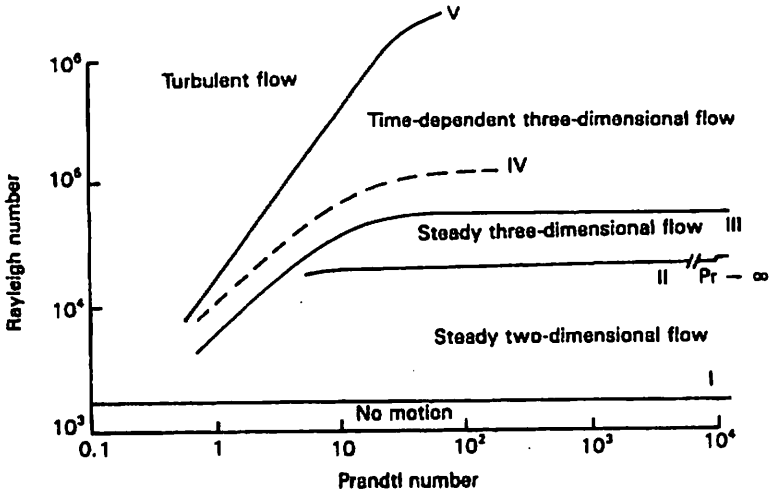

Figure 6.11. Flow Regimes in a Horizontal Fluid Layer Heated From Below, Gebhart, et al. (1988); original from Krishnamurti (1970).

References

Castaing, B., G. Gunaratno, F. Heslot, L. Kadanoff, A. Libchaber, S. Thomae, X.-Z. Wu, S. Zaleski, and G. Zanetti, "Scaling of hard thermal turbulence in Rayleigh-B´ nard convection," J. Fluid Mech. 204 1-30 (1989).

Chien, K.-Y., "Predictions of channel and boundary layer flow swith a low-Reynolds-number two-equation model of turbulence, AIAA-80-0134 (1980); AIAA J 20 33-38 (1982).

Elder, J. W., J. Fluid Mech. 23 99 (1965).

Gebhart, B., Juluria, Y., Mahajan, R. L., Sammakia, B., *Buoyancy-induced Flows and Transport,* Hemisphere, Washington, D.C., 1988.

Henkes, R. A. W. M. and C. J. Hoogendoorn, "On the stability of the natural convection flow in a square cavity heated from the side," Appl. Sci. Res. 47 195-220 (1990).

Henkes, R. A. W. M., F. F. Vander Vlugt, and C. J. Hoogendoorn, "Natural -convection flow in a square cavity calculated with low-Reynolds-number turbulence models," Int. J. Heat Mass Transfer 34 377-388 (1991).

Henkes, R. A. W. M. and C. J. Hoogendoorn, "Comparison of turbulence models for the natural convection boundary layer along a heated vertical plate," Int. J. Heat Mass Transf. 32 157-169 (1989). See also "Letters to the Editors", 36 245-247 (1993).

Heslot, F., B. Castaing, and A. Libchaber, "Transitions to turbulence in helium gas," Phys. Rev. A 36 5870-5873 (1987).

Ivey, G. N., "Experiments on transient natural convection in a cavity," J. Fluid Mech. 144 389-401 (1984).

Janssen, R. J. A. and R. A. W. M. Henkes, "Accuracy of Finite-Volume Discretizations for the Bifurcating Natural-Convection Flow in a Square Cavity," Num. Heat Trans., B24 191-207 (1993).

Jones, W. P. and B. E. Launder, "The prediction of laminarization with a two-equation model of turbulence, Int. J. Heat Mass Transfer 15 301-314 (1972).

Kadanoff, L. P., "Scaling and Structures in the Hard Turbulence Region of Rayleigh B´ nard Convection," Ch. 9, pp. 263-269 in *New Perspectives in Turbulence*, Sirovich, L. (ed), Springer-Verlag (1991).

Kerr, R. M., "Rayleigh number scaling in numerical convection," J. Fluid Mech. 310 139-179 (1996).

Krishnamurti, R., J. Fluid Mech. 42 295 (1970).

Lage, J. L. and A. Bejan, "The Ra-Pr Domain of Laminar Natural Convection in an Enclosure Heated from the Side," Num. Heat Trans., A21 21-41 (1991).

Laufer, J., "The structure of turbulence in fully developed pipe flow," NACA Tech. Rept. No. 1174 (1954)

Le Qué ré , P., "Accurate Solutions to the Square Thermally Driven Cavity at High Rayleigh Number," Computers Fluids 20 29-41 (1991).

Liu, F. and J. X. Wen, "Development and validation of an advanced turbulence model for buoyancy driven flows in enclosures," Int. J. Heat Mass Transfer 42 3967-3981 (1999).

Malkus, W. V. R., and Veronis, G., J. Fluid Mech. 4 225 (1958).

McLaughlin, J. B., and S. A. Orszag, "Transition from periodic to chaotic thermal convection," J. Fluid Mech. 122 123-142 (1982).

Paolucci, S. and D. R. Chenoweth, "Transition to chaos in a differentially heated vertical cavity," J. Fluid Mech. 201 379-410 (1989).

Peeters, T. W. J. and R. A. W. M. Henkes, "The Reynolds-stress model of turbulence applied to the natural-convection boundary layer along a heated vertical plate," Int. J. Heat Mass Transfer 35 403-420 (1992).

Pironneau, O., "Modeles numériques pour les écoulements turbulents dans des géométries complexes," C. R. Acad. Sci., Paris, 327, Sec. II.b. 325-331 (1999).

Prasad, A. K., "Numerical Simulation of Non-penetrative Turbulent Thermal Convection," Num. Heat Trans., Part A, 35 451-466 (1999).

Rosensweig, R. E., *Ferrohydrodynamics*, Cambridge University Press (1985); Dover(1998).

Schlichting, H. (trans. J. Kestin), Boundary layer Theory, McGraw-Hill, New York (1960).

Tagawa, T. and H. Ozoe, "Effect of Prandtl Number and Computational Schemes on the Oscillatory Natural Convection in an Enclosure," Num. Heat Trans., A30 271-282 (1996).

Versteegh, T. A. M. and F. T. M. Nieuwstadt, "A direct numerical simulation of natural convection between two infinite vertical differentially heated walls scaling laws and wall functions," (sic) Int. J. Heat Mass Transfer 42 3673-3693 (1999).

Zahn, M. and L. L. Pioch, "Magnetizable Fluid Behavior With Effective Positive, Zero or Negative Dynamic Viscosity: A Study of Non-symmetric Stress Tensors", Symp. Recent Trents Sci. Tech. Magnetic Fluids, Oct. 16-18, 1997, India.

Zahn, M. and D. R. Greer, "Ferrohydrodynamic pumping in spatially uniform sinusoidally time-varying magnetic fields," J. Mag. Mag. Mat. 149 165-173 (1995).